

Constraining annihilating Dark Matter with the Cosmic Microwave Background

Aaron C. Vincent

IFIC (Universitat de València — CSIC)

12 March 2013

Based on arXiv:1303.xxxx [hep-ph],
with **Laura Lopez-Honorez** (Vrije U. Brussels),
Olga Mena (IFIC) ,
Sergio Palomares-Ruiz (IFIC / UT Lisboa)

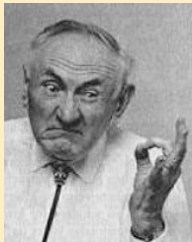
Outline

- 1 Why Annihilating Dark Matter?
- 2 Why the CMB?
- 3 DM vs CMB
- 4 Analysis and Results
- 5 Conclusions

I. Why Dark Matter

The dark matter paradigm, allows the explanation of phenomena on many scales:

First observations by Zwicky (1930's) of proper motions of galaxies within the Coma **Cluster** imply large mass/luminosity.



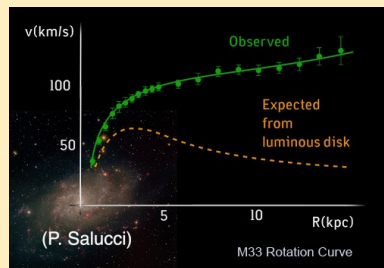
I. Why Dark Matter

The dark matter paradigm, allows the explanation of phenomena on many scales:

First observations by Zwicky (1930's) of proper motions of galaxies within the Coma **Cluster** imply large mass/luminosity.

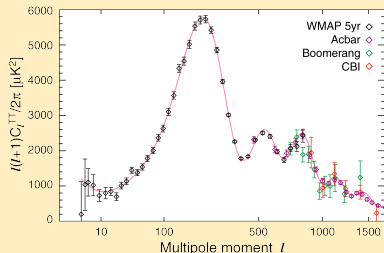


1970's: Ruben et al. find that rotation curves of gases in **galaxies** are too fast for visible mass



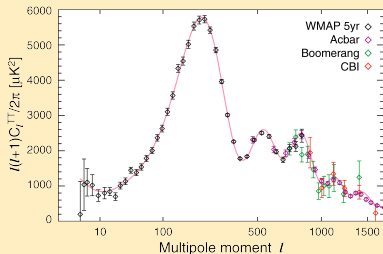
(an incomplete list of) further evidence

Cosmic microwave background
(**CMB**) observations imply a
large non-baryonic matter
component to account for
acoustic oscillations.



(an incomplete list of) further evidence

Cosmic microwave background (CMB) observations imply a large non-baryonic matter component to account for acoustic oscillations.



Gravitational lensing, in particular of colliding clusters implies separate baryonic and lensing components.



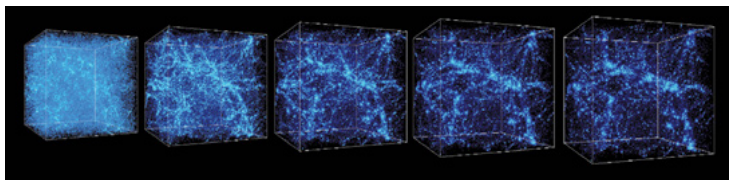
(image: not the bullet cluster!)

What is dark matter?

From gravity, we know it must have

- Galaxies + CMB: very **small self-interaction** cross-section (to form “fluffy” structures);
- CMB, lensing: Very **small interaction with the SM** ;
- CMB, LSS: Massive enough to be **non-relativistic** (CDM) or **mildly relativistic** (WDM) at decoupling;
- Abundance (where $\Omega_i = \rho_i/\rho_c$):

$$\Rightarrow \frac{\Omega_{DM}}{\Omega_{SM}} = \frac{0.111h^{-2}}{0.0226h^{-2}} = 4.9$$



Particle nature: the WIMP miracle

Freeze-out abundance ($\rho_{DM} \simeq \rho_{SM}$) depends on the **self-annihilation** rate. To get the proper abundance of DM today, we need a self-annihilation cross-section:

$$\langle\sigma v\rangle \simeq 3 \times 10^{-26} \text{cm}^3 \text{s}^{-1}$$

...which is about the same cross-section as processes interacting via the **electroweak force**.

This prompts speculation that DM could be a “**weakly interacting massive particle**” (**WIMP**)

Particle nature: the WIMP miracle

Freeze-out abundance ($\rho_{DM} \simeq \rho_{SM}$) depends on the **self-annihilation** rate. To get the proper abundance of DM today, we need a self-annihilation cross-section:

$$\langle\sigma v\rangle \simeq 3 \times 10^{-26} \text{cm}^3 \text{s}^{-1}$$

...which is about the same cross-section as processes interacting via the **electroweak force**.

This prompts speculation that DM could be a “**weakly interacting massive particle**” (**WIMP**)

Whatever the channel, a thermal origin implies ongoing interaction between WIMPs, from decoupling to the present-day halos.

Could we see such a signature?

what do we know about DM's particle properties?

- **Direct detection** experiments search for nuclear recoils caused by DM-SM collisions
- **Collider searches** (i.e. LHC) look for missing energy from collisions
- **Indirect searches** give us a multitude of opportunities:
 - Direct annihilation signals: dwarf galaxies, the GC (e.g. Fermi line)
 - Diffuse gamma rays
 - Neutrinos from the sun
 - Intergalactic heating
 - Excess antimatter (positrons, anti-deuterons, etc.)
 - the CMB...

II: The Cosmic Microwave Background

The CMB anisotropies (in two slides)

- After the end of inflation, different regions of the universe slowly began to causally reconnect.

II: The Cosmic Microwave Background

The CMB anisotropies (in two slides)

- After the end of inflation, different regions of the universe slowly began to causally reconnect.
- As gravitational perturbations from inflation reenter the horizon, they seed oscillations in the photon baryon fluid.

II: The Cosmic Microwave Background

The CMB anisotropies (in two slides)

- After the end of inflation, different regions of the universe slowly began to causally reconnect.
- As gravitational perturbations from inflation reenter the horizon, they seed oscillations in the photon baryon fluid.
- The power spectrum of these oscillations comes from the primordial perturbations, while the oscillations are maintained by gravity from the matter component, and pressure from baryons and photons.

II: The Cosmic Microwave Background

The CMB anisotropies (in two slides)

- After the end of inflation, different regions of the universe slowly began to causally reconnect.
- As gravitational perturbations from inflation reenter the horizon, they seed oscillations in the photon baryon fluid.
- The power spectrum of these oscillations comes from the primordial perturbations, while the oscillations are maintained by gravity from the matter component, and pressure from baryons and photons.
- At high temperatures, the photons and baryons are tightly coupled.

II: The Cosmic Microwave Background

The CMB anisotropies (in two slides)

- After the end of inflation, different regions of the universe slowly began to causally reconnect.
- As gravitational perturbations from inflation reenter the horizon, they seed oscillations in the photon baryon fluid.
- The power spectrum of these oscillations comes from the primordial perturbations, while the oscillations are maintained by gravity from the matter component, and pressure from baryons and photons.
- At high temperatures, the photons and baryons are tightly coupled.
- As expansion forces the fluid to cool, hydrogen recombines. Once $T \sim 0.1 \times 13.6$ eV, photons can no longer excite H atoms. They **decouple**, streaming away until the present.

- **Hot**, overdense regions emit higher-energy photons
- However, these are **redshifted** by the gravitational potential they escape (**Sachs-Wolfe** effect)
- Photons are further **doppler** shifted due to their relative motion
- **Integrated Sachs-Wolfe** causes further red/blue shifting.

$$\Theta|_{\text{obs}} = \underbrace{(\Theta_0 + \psi)|_{\text{dec}}}_{\text{SW}} + \underbrace{\hat{n} \cdot \vec{v}_b|_{\text{dec}}}_{\text{Doppler}} + \underbrace{\int_{\eta_{\text{dec}}}^{\eta_0} d\eta (\phi' + \psi')}_{\text{ISW}}$$

- **Hot**, overdense regions emit higher-energy photons
- However, these are **redshifted** by the gravitational potential they escape (**Sachs-Wolfe** effect)
- Photons are further **doppler** shifted due to their relative motion
- **Integrated Sachs-Wolfe** causes further red/blue shifting.

$$\Theta|_{\text{obs}} = \underbrace{(\Theta_0 + \psi)|_{\text{dec}}}_{\text{SW}} + \underbrace{\hat{n} \cdot \vec{v}_b|_{\text{dec}}}_{\text{Doppler}} + \underbrace{\int_{\eta_{\text{dec}}}^{\eta_0} d\eta (\phi' + \psi')}_{\text{ISW}}$$

CMB photons have a **long way** to travel from last scattering. What if there's an extra source of energy along the way from DM? Will it increase their chance of rescattering? **Can we detect it?**

III. Energy deposition into the IGM from annihilating DM

The energy **injected** into the IGM is quite straightforward

$$\begin{aligned}\left(\frac{dE}{dVdt}\right)_{\text{injected}} &= m_\chi n_\chi(z)^2 \langle \sigma v \rangle \\ &= (1+z)^6 (\Omega_{DM} \rho_c)^2 \frac{\langle \sigma v \rangle}{m_\chi},\end{aligned}$$

III. Energy deposition into the IGM from annihilating DM

The energy **injected** into the IGM is quite straightforward

$$\begin{aligned}\left(\frac{dE}{dVdt}\right)_{\text{injected}} &= m_\chi n_\chi(z)^2 \langle \sigma v \rangle \\ &= (1+z)^6 (\Omega_{DM} \rho_c)^2 \frac{\langle \sigma v \rangle}{m_\chi},\end{aligned}$$

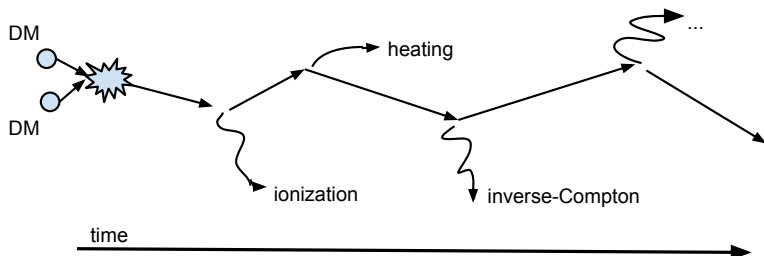
Deposited energy is a different story

- Final-state invisible particles (e.g. **neutrinos**) do not heat the IGM
- Deposition efficiency will depend on the transparency of the IGM to the daughter particles i at each redshift z and energy E_i .
- Heating and ionization are due to electromagnetic processes.
Therefore the final states that matter are **electrons**, **positrons** and **photons**.

Energy deposition into the IGM

Proper calculation of the deposition efficiency

- 1 At a given redshift z , calculate the final-state spectrum dN_i/dE_i for $i = \{e^+, e^-, \gamma\}$
- 2 Calculate the energy loss to (inverse) Compton scattering, Coulomb scattering, (photo) ionization or pair-production for each species.
- 3 Step forward to the next value of z , given the new $E_i = E_{i,0} - E(z)'dz$, including loss to **IGM** and to **redshift**.
- 4 Repeat.



Energy deposition into the IGM

From this process, one can build a transfer matrix $T_i(z', z, E_i)$ (Slatyer 2012) which gives the fraction of the initial energy E_i **injected** at redshift z' that is **deposited** into the IGM at redshift z . Then we can rewrite our previous equation:

$$\left(\frac{dE}{dVdt} \right)_{\text{deposited}} = f(z, m_\chi) (1+z)^6 (\Omega_{DM} \rho_c)^2 \frac{\langle \sigma v \rangle}{m_\chi}, \quad (1)$$

Energy deposition into the IGM

From this process, one can build a transfer matrix $T_i(z', z, E_i)$ (Slatyer 2012) which gives the fraction of the initial energy E_i **injected** at redshift z' that is **deposited** into the IGM at redshift z . Then we can rewrite our previous equation:

$$\left(\frac{dE}{dVdt}\right)_{\text{deposited}} = f(z, m_\chi)(1+z)^6(\Omega_{DM}\rho_c)^2\frac{\langle\sigma v\rangle}{m_\chi}, \quad (1)$$

where

$$f(z, m_\chi) = \frac{\sum_i \int dz' \frac{(1+z')^2}{H(z')} \int T_i(z', z, E_i) E_i \frac{dN}{dE_i} dE_i}{\frac{(1+z)^3}{H(z)} \sum_i \int E \frac{dN_i}{dE_i}(m_\chi) dE_i}$$

Numerator: properly computed energy deposition.

Denominator: normalization to (1).

Energy deposition into the IGM

From this process, one can build a transfer matrix $T_i(z', z, E_i)$ which gives the fraction of the initial energy E_i **injected** at redshift z' that is **deposited** into the IGM at redshift z . Then we can rewrite our previous equation:

$$\left(\frac{dE}{dVdt}\right)_{\text{deposited}} = f(z, m_\chi)(1+z)^6(\Omega_{DM}\rho_c)^2\frac{\langle\sigma v\rangle}{m_\chi},$$

where

$$f(z, m_\chi) = \frac{\sum_i \int dz' \frac{(1+z')^2}{H(z')} \int T_i(z', z, E_i) E_i \frac{dN}{dE_i}(m_\chi) dE_i}{\frac{(1+z)^3}{H(z)} \sum_i \int E \frac{dN_i}{dE_i}(m_\chi) dE_i}$$

Time \leftrightarrow redshift;

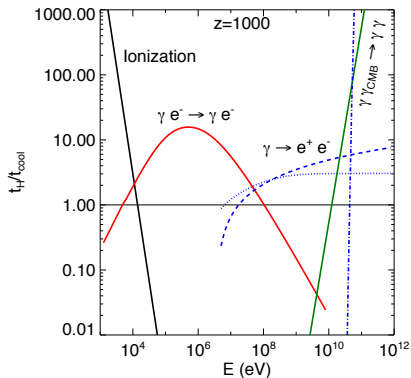
Injected energy spectrum from annihilation;

Physics of the intergalactic medium.

Energy deposition into the IGM

The energy deposition efficiency depends on *energy* and *redshift*

$$\left(\frac{dE}{dVdt} \right)_{\text{deposited}} = f(z, m_\chi) (1+z)^6 (\Omega_{DM} \rho_c)^2 \frac{\langle \sigma v \rangle}{m_\chi}$$

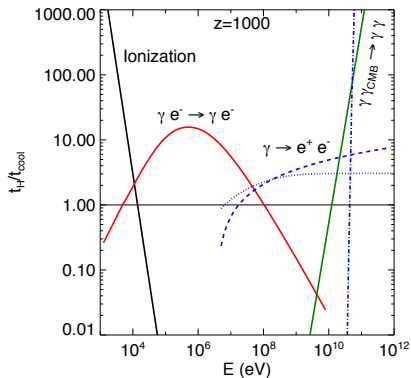


Slatyer et al. 2009

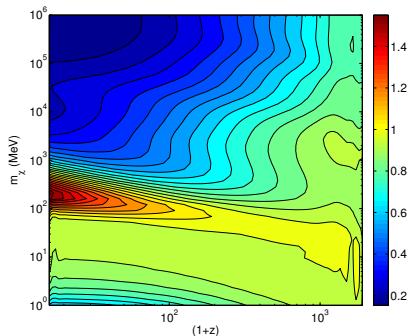
Energy deposition into the IGM

The energy deposition efficiency depends on *energy* and *redshift*

$$\left(\frac{dE}{dVdt}\right)_{\text{deposited}} = f(z, m_\chi)(1+z)^6(\Omega_{DM}\rho_c)^2 \frac{\langle\sigma v\rangle}{m_\chi}$$



Slatyer et al. 2009



$f(z, m_\chi)$

Energy injection effect on CMB photons

Extra deposited energy causes **heating** and **ionization**:

$$\begin{aligned}\frac{dT_m}{dz} &= -\frac{1}{(1+z)H(z)} \frac{2}{3k_B} \frac{g_h(z)}{N_H(z)[1+f_{\text{He}}+X_e]} \left(\frac{dE}{dtdV}\right)_{\text{deposited}} ; \\ \frac{dN_{\text{Is}}^{\text{HI}}}{dz} &= \frac{1}{(1+z)H(z)} \frac{1}{N_H(z)[1+f_{\text{He}}]} \frac{\tilde{g}_{\text{ion}}^{\text{H}}(z)}{E_{\text{ion}}^{\text{HI}}} \left(\frac{dE}{dtdV}\right)_{\text{deposited}} ; \\ \frac{dN_{\text{Is}}^{\text{HEI}}}{dz} &= \frac{1}{(1+z)H(z)} \frac{f_{\text{He}}}{N_H(z)[1+f_{\text{He}}]} \frac{\tilde{g}_{\text{ion}}^{\text{He}}(z)}{E_{\text{ion}}^{\text{HEI}}} \left(\frac{dE}{dtdV}\right)_{\text{deposited}} .\end{aligned}$$

f_{He} Helium fraction;
 E_{ion}^i ionization potential;
 g_h, g_{ion}^i heating and ionization efficiencies.

Early Times: The ionization floor

- Dark matter annihilation rate is proportional to $(1+z)^6$, which leads to a dependence of

$$\sqrt{1+z} \quad (2)$$

for the heating and ionization rates. Therefore dominates in the early Universe. Around $z = 1100$, the extra energy injection has the effect of **delaying recombination**.

Early Times: The ionization floor

- Dark matter annihilation rate is proportional to $(1+z)^6$, which leads to a dependence of

$$\sqrt{1+z} \quad (2)$$

for the heating and ionization rates. Therefore dominates in the early Universe. Around $z = 1100$, the extra energy injection has the effect of **delaying recombination**.

- This **broadens the last scattering surface**. This can be seen as a broadening of the CMB's "focal plane": you can still resolve large structures, but smaller details become blurred: \Rightarrow **suppression of the correlations at high multipoles**.

Early Times: The ionization floor

- Dark matter annihilation rate is proportional to $(1+z)^6$, which leads to a dependence of

$$\sqrt{1+z} \quad (2)$$

for the heating and ionization rates. Therefore dominates in the early Universe. Around $z = 1100$, the extra energy injection has the effect of **delaying recombination**.

- This **broadens the last scattering surface**. This can be seen as a broadening of the CMB's "focal plane": you can still resolve large structures, but smaller details become blurred: \Rightarrow **suppression of the correlations at high multipoles**.
- This is **degenerate** with a change in the scalar spectral index n_s .

Early Times: The ionization floor

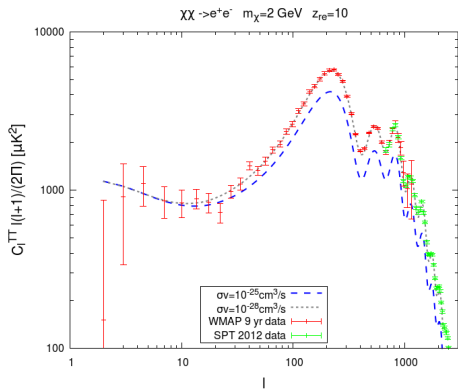
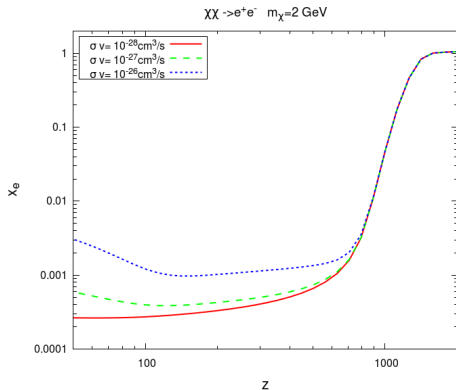
- Dark matter annihilation rate is proportional to $(1+z)^6$, which leads to a dependence of

$$\sqrt{1+z} \quad (2)$$

for the heating and ionization rates. Therefore dominates in the early Universe. Around $z = 1100$, the extra energy injection has the effect of **delaying recombination**.

- This **broadens the last scattering surface**. This can be seen as a broadening of the CMB's "focal plane": you can still resolve large structures, but smaller details become blurred: \Rightarrow **suppression of the correlations at high multipoles**.
- This is **degenerate** with a change in the scalar spectral index n_s .
- This can be disentangled by late-time effects.

Early Times: The ionization floor



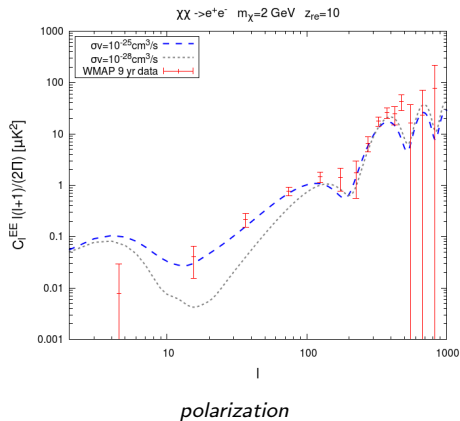
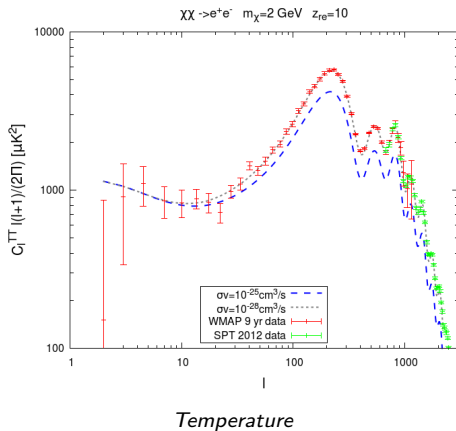
Continuous energy injection from DM at late times ($z < 40$) can:

- Increase the **optical depth** of the universe, given more free ions for the CMB photons to scatter on.

Continuous energy injection from DM at late times ($z < 40$) can:

- Increase the **optical depth** of the universe, given more free ions for the CMB photons to scatter on.
- Affect the reionization history, which changes the **polarization** spectrum. Rescattering at low redshift:
 - Decreases polarization (as well as temperature) correlations on small scales (large l)
 - Increases polarization correlations on large scales ($l \sim 2 - 200$) since only certain polarizations are rescattered toward us (like the sky).

Late times



Late times: the influence of Halos

In spite of the $(1+z)^6$ suppression at late times, there is an effect which enhances the annihilation rate of dark matter at late time: the **formation of halos**:

Late times: the influence of Halos

In spite of the $(1+z)^6$ suppression at late times, there is an effect which enhances the annihilation rate of dark matter at late time: the **formation of halos**:

$$n^2 \propto \int dM \frac{dN_{halos}}{dM}(z, M) \tilde{g}(c_\Delta(M, z)) \frac{M \Delta \rho_c(z)}{3}.$$

- $\frac{dN_{halos}}{dM}(z, M)$: halo mass function
- $\tilde{g}(c_\Delta(M, z)) \frac{M \Delta \rho_c(z)}{3}$: enhancement of individual halos of mass M .
Computed by integrating over an NFW profile:

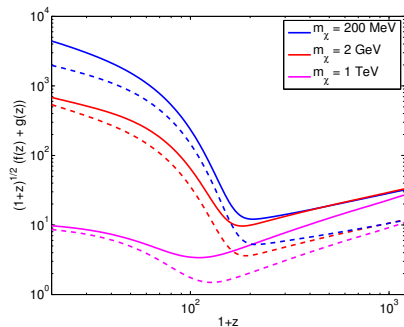
$$\int_0^{r_\Delta} dr 4\pi r^2 \rho_{NFW}^2(r) = \tilde{g}(c_\Delta) \frac{M \Delta \rho_c(z)}{3};$$

$$\rho_{NFW}(r) = \rho_s \frac{4}{(r/r_s)(1+r/r_s)^2}$$

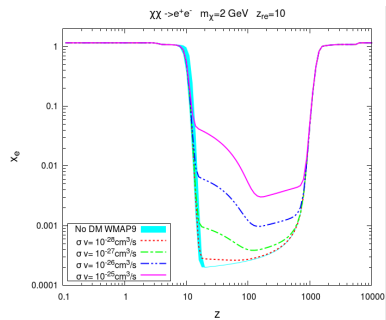
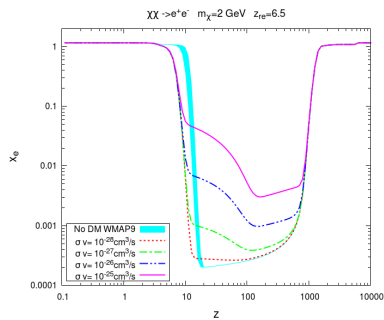
Late times: the influence of Halos

$$n^2 \propto \int dM \frac{dN_{halos}}{dM}(z, M) \tilde{g}(c_{\Delta}(M, z)) \frac{M \Delta \rho_c(z)}{3}.$$

For the halo mass function $\frac{dN_{halos}}{dM}(z, M)$, we use a parametrization of the results from the Multidark (BigBolshoi) simulation:



Full effect on the ionization history



IV: Analysis

To properly constrain the DM cross-section, we perform a full Monte-Carlo for each m_χ over:

Ω_b	the baryonic content of the Universe;
Ω_{CDM}	the dark matter content of the Universe;
z_{reio}	the time of reionization;
n_s	the scalar spectral index;
A_s	the primordial power spectrum;
$\langle\sigma v\rangle$	the DM self-annihilation cross-section.

For the numerics, we use CAMB, CosmoRec with CosmoMC for the Monte-Carlo.

This allows us to extract 2σ (95% c.l.) constraints on the thermally-averaged cross-section.

We use the following data:

- Nine-year WMAP CMB data;
- South Pole Telescope (Dec. 2012) CMB data;
- BAO measurements from BOSS DR9, LRG (DR7) 6dF Galaxy Survey and WiggleZ (different redshifts);
- Hubble Space Telescope (constraints on H_0).

...and nuisance parameters:

- Sunyaev–Zel'dovich contribution A_{SZ} ;
- Amplitude of clustered point-source contribution A_C ;
- Amplitude of Poisson-distributed point sources A_P .

The Model

We consider two channels of self-annihilating dark matter:

$$\chi\chi \rightarrow e^+e^-$$

and

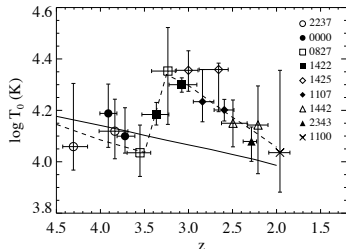
$$\chi\chi \rightarrow \mu^+\mu^-$$

These “leptophilic” channels will be the **most constrained**, since IGM heating is an **electromagnetic** process. Also interesting because they have been invoked to explain “anomalies” observed by PAMELA (high-E e^+), INTEGRAL (low-E e^+) and ARCADE (excess diffuse radio from synchrotron).

For many more channels see *e.g.* estimates by Cline & Scott 2013.

Further constraints: T_{IGM}

The matter temperature of the intergalactic medium at redshifts 2 – 5 has been measured by Ly- α observations:



Schaye et al. 2000

This can be used (e.g. *Cirelli et al 2009*) to constrain the amount of energy injected by DM.

Further constraints: the Gunn-Peterson observations

Lyman- α observations also tell us that:

- At $z \gtrsim 6$, the universe was not yet fully ionized ($X_H \gtrsim 10^{-3}$)
- By $z = 5.5$, reionization was nearly complete ($X_H \lesssim 10^{-4}$)

Further constraints: the Gunn-Peterson observations

Lyman- α observations also tell us that:

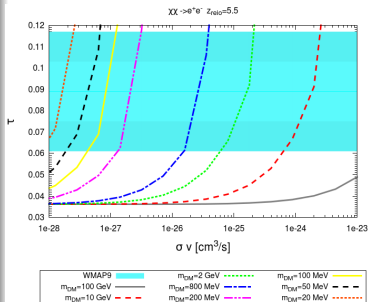
- At $z \gtrsim 6$, the universe was not yet fully ionized ($X_H \gtrsim 10^{-3}$)
 - By $z = 5.5$, reionization was nearly complete ($X_H \lesssim 10^{-4}$)
- This is in **conflict** with WMAP measurements of the reionization optical depth τ , which favour $z_{\text{reio}} \sim 10$.

Further constraints: the Gunn-Peterson observations

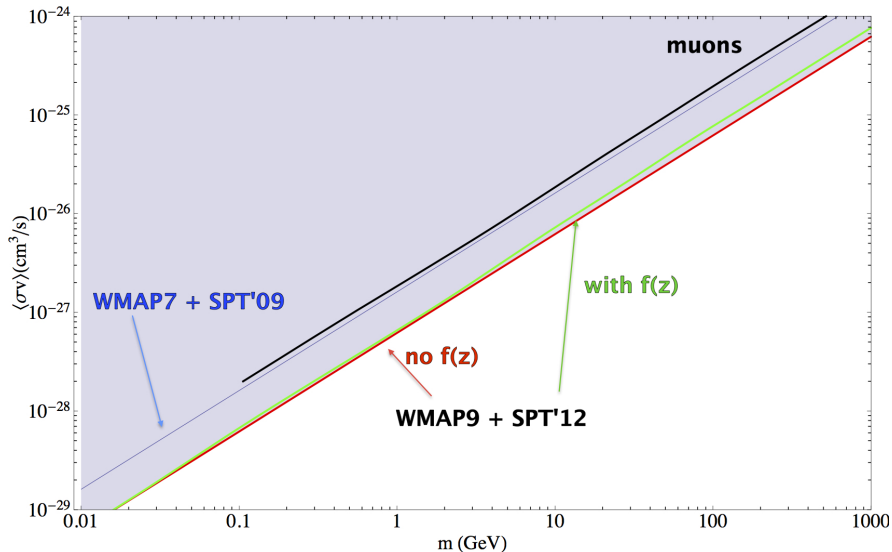
Lyman- α observations also tell us that:

- At $z \gtrsim 6$, the universe was not yet fully ionized ($X_H \geq 10^{-3}$)
- By $z = 5.5$, reionization was nearly complete ($X_H \leq 10^{-4}$)

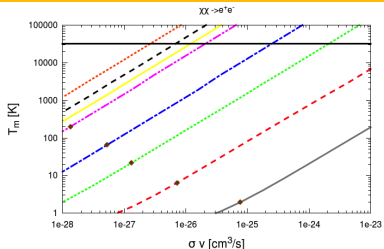
- This is in **conflict** with WMAP measurements of the reionization optical depth τ , which favour $z_{\text{reio}} \sim 10$.
- However, annihilating dark matter can increase τ , bringing WMAP and Gunn-Peterson observations back into agreement!
(see *e.g. Lesgourgues 2012*)
- Unfortunately, the values of $\langle \sigma v \rangle$ required to do so are, we will see, **badly excluded**



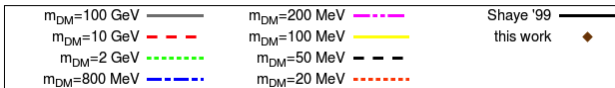
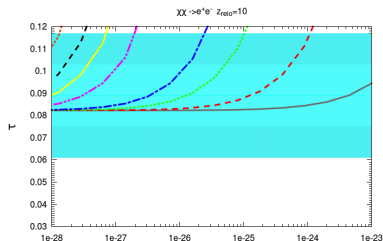
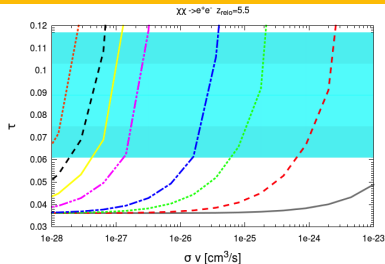
Results



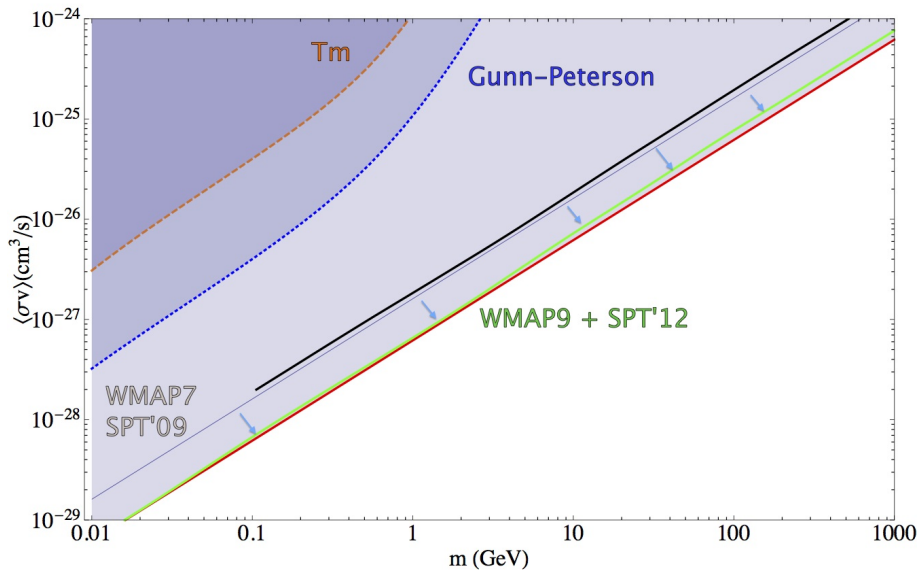
Results: T_m and τ (Top: $z_{\text{reio}} = 5.5$; Bottom: $z_{\text{reio}} = 10$)



(T from reionization not included)



Results: all together



Results: Salient points

- Improvement by a factor of ~ 3 over WMAP7/SPT'09 bounds.
- T_m , Gunn-Peterson bounds less constraining than CMB temperature and polarization data
- This means that early universe (broadening of last scattering surface) effects dominate over late-time (halo formation) effects
- Gunn-Peterson and WMAP cannot be brought back into agreement by using allowed $(m_\chi, \langle\sigma v\rangle)$ combinations.

V. Conclusions

- We have explored the effect of annihilating dark matter on the CMB temperature and polarization power spectra.
- We have included a full description of time- and energy-dependent deposition of DM energy into the IGM.
- Improved constraints by using CMB (WMAP9 + SPT), Ly- α (T and τ) and BAO surveys.
- Excluded annihilating $\chi\chi \rightarrow e^+e^-$ with the thermal abundance cross-section for $m_\chi \lesssim 30$ GeV.
- Ibid. for $\chi\chi \rightarrow \mu^+\mu^-$ for $m_\chi \lesssim 10$ GeV.
- t minus 1 week for Planck data: let's see what they have in store for us!

Parameter	Prior
$\Omega_b h^2$	0.005 \rightarrow 0.1
$\Omega_c h^2$	0.01 \rightarrow 0.99
Θ_s	0.5 \rightarrow 10
z_{reio}	6 \rightarrow 12
n_s	0.5 \rightarrow 1.5
$\ln(10^{10} A_s)$	2.7 \rightarrow 4
$\langle \sigma v \rangle / (3 \cdot 10^{-26} \text{cm}^3/\text{s})$	$10^{-5} \rightarrow 10^{2.5}$

Table: *Uniform priors for the cosmological parameters considered here.*

halo mass function

